Available online at www.sciencedirect.com
SCIENCE DIRECT®
Journal of Molecular Structure 700 (2004) 29–38
Journal of MOLECULAR STRUCTURE
www.elsevier.com/locate/molstruc

A simple method for the characterization of OHO-hydrogen bonds by ^{1}H-solid state NMR spectroscopy

Th. Emmler, S. Gieschler, H.H. Limbach, G. Buntkowsky*

Institut für Chemie, Freie Universität Berlin, Takustraβe 3, 14195 Berlin, Germany

Received 19 December 2003; revised 29 January 2004; accepted 29 January 2004

Abstract

A set of OHO hydrogen bonded systems with known neutron diffraction structure has been studied by fast ^{1}H-MAS echo spectroscopy. It is shown that the application of a simple rotor synchronized echo sequence combined with fast MAS allows a faithful determination of the chemical shift of the proton in the hydrogen bond. Employing the empirical valence bond order model, the experimental ^{1}H chemical shifts of the hydrogen bonded protons are correlated to the hydrogen bond geometries. The resulting correlation between the proton chemical shift and the deviation of the proton from the center of the hydrogen bond covers a broad range of substances. Deviations from the correlation curve, which are observed in certain systems with strong hydrogen bonds, are explained in terms of proton tautomerism or delocalization in low-barrier hydrogen bonds. These deviations are a highly diagnostic tool to select potential candidates for further experimental and theoretical studies. Thus, the combination of the ^{1}H-MAS echo sequence with the correlation curve yields a simple and versatile tool for the structural analysis of OHO hydrogen bonds.
© 2004 Elsevier B.V. All rights reserved.

Keywords: ^{1}H-MAS; Hydrogen bonds; OHO; Hydrogen bond correlation

Hydrogen bonding is one of the major structure and function determining phenomenon in bio-organic molecules in solution and solids [1]. Whereas, the geometry of crystalline compounds can be studied by X-ray and neutron diffraction, NMR spectroscopy has become a major tool in the study of biomolecules in liquids and non-crystalline solids. In order to determine hydrogen bond geometries by NMR, the NMR parameters have to be 'translated' into distance information. The most straightforward way is to measure dipolar couplings by solid state NMR, which are proportional to the average inverse cubic distances of nuclear spin pairs. If one wants to measure dipolar couplings to ^{1}H, care must be taken to remove the homonuclear dipolar ^{1}H– ^{1}H coupling. Thus, Griffin et al. [2] have measured the dipolar ^{15}N–H-couplings in NHO-hydrogen bonded systems, employing non-spinning or slow spinning under the magic angle (MAS), which were converted to NH-distances. Some of us have proposed to study dipolar ^{15}N–D couplings instead [3], a method which has been recently successfully applied to study the geometries of NHN- [4] and NHO-hydrogen bonds [5] by solid state NMR of static samples. This method is also applicable to MAS-conditions [6].

Unfortunately, dipolar couplings are averaged in the liquid state or are not accessible in many important OHO-hydrogen bonded systems. Since the chemical shifts of hydrogen bonded protons or of the heavy atoms of hydrogen bonds are strongly dependent on the proton position, correlations between NMR parameters and hydrogen bond geometries have been successfully established as an alternative pathway for the structural analysis of the hydrogen bond. In these cases, high-resolution solid state ^{1}H NMR spectroscopy is the preferred NMR method. This technique has made major progresses by the development of fast ^{1}H MAS techniques and the availability of high magnetic fields. Nowadays, MAS frequencies of 20 kHz and above are routinely available, even in a non-dedicated solid state NMR laboratory and it is in general no longer necessary to employ cumbersome homonuclear decoupling techniques like CRAMPS [35] and related schemes for high-resolution ^{1}H MAS–NMR spectroscopy. As a result of these technical developments, high resolved proton MAS–NMR spectra are nowadays obtainable with any standard highfield NMR spectrometer equipped with a fast MAS

* Corresponding author. Fax: +49-30-838-55310.
E-mail address: bunt@chemie.fu-berlin.de (G. Buntkowsky).

0022-2860/$ - see front matter © 2004 Elsevier B.V. All rights reserved.
doi:10.1016/j.molstruc.2004.01.045

probe. In the case of OHO-hydrogen bonds, Sternberg [7] and McDermott [8] have proposed ^{1}H chemical shift-geometry correlations, based on ^{1}H solid state NMR measurements and neutron crystallography structures. These correlations are already used for the characterization of strong and short hydrogen bonds in biological systems by NMR studies of Mildvan et al. [9,10]. For a recent review, we refer to a paper of Brunner et al. [11]. In the case of NHN- and NHO- systems, some of us have found a chemical shift-NH-distance correlation for various systems [4,5] which filled especially the gap of short and strong hydrogen bonds. These correlations have been applied successfully to hydrogen bonds in the liquid state [12,13].

Whereas it had been recognized early that the short distances r_{AH} of hydrogen bonded systems of the type A–H···B increases when the heavy atom distance r_{AB} is decreased (Fig. 1) [14], recently it was realized by Steiner et al. for OHO-systems [15], NHN-systems [16] and NHO- and other systems [17] that in fact the correlation is superior for the two heavy atom-hydrogen distances r_{AH} and r_{HB}, which are, however, more difficult to measure. Note, that the hydrogen bond angle α does not play a role in these correlations since this information is already included indirectly in the two bond lengths.

At room temperature, protons in hydrogen bonds are often delocalized and can no longer be associated with a single position in the hydrogen bond. As a consequence, any correlation will break down.

A large part of the success of a correlation has to be attributed to recent developments in neutron crystallography and the availability of low-temperature neutron diffraction data in the Cambridge Structural Database (CSD). A first theoretical explanation of the r_{AH} vs. r_{HB} correlation was provided by Steiner [16,17] in terms of the empirical valence bond order model of Brown [18], which is based on the valence bond concept of Pauling [21]. Using various quantum-mechanical methods these empirical valence bond order correlations were quantitatively reproduced [4,19,20].

The scope of this paper is therefore, to demonstrate that the combination of fast ^{1}H MAS–NMR echo spectroscopy with the ^{1}H chemical shift-geometry correlation, parameterized by the valence bond order model allows a faithful characterization of the geometrical structure of OHO-hydrogen bonds. For this purpose it is necessary to enlarge the experimental database of the ^{1}H chemical shift-geometry correlation for OHO-hydrogen bonds, based on low-temperature neutron structures contained in the CSD and characterize their chemical shift by high-resolution ^{1}H solid state MAS–NMR echo spectroscopy.

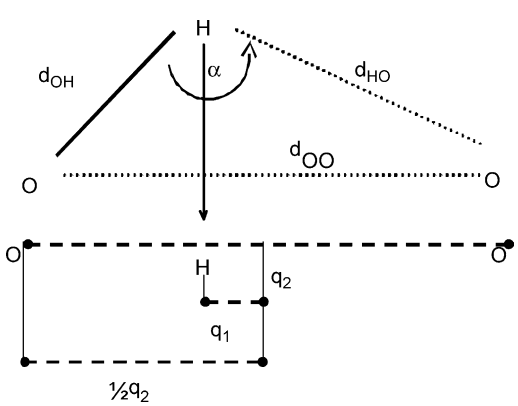

Fig. 1. Geometric parameters of a hydrogen bond A–H···B. For a linear hydrogen bond q_2 coincides with the heavy atoms distance.

In particular, we are interested to elucidate whether the valence bond order model is able to distinguish between normal deviations of experimental geometries from the hydrogen bond correlation (arising from the usual scattering of the data) to deviations caused by a delocalization of the proton in the hydrogen bond, which is still difficult to establish experimentally. If the latter were the case, solid state ^{1}H MAS–NMR would provide a simple method for detecting compounds with interesting H-bond properties, which could be studied in a second phase by low-temperature ^{2}H NMR down to 10 K.

The rest of this paper is organized as follows: after a brief introduction into the selected substances and the experimental methods, a short review of the valence bond order concept for hydrogen bond correlations is given. This review is followed by the experimental results and their discussion.

1. Materials and methods

1.1. Substances

A careful selection of the model compounds with known structure was necessary for a reliable correlation between ^{1}H-chemical shift and the proton position. To avoid systematic deviations it was advisable to employ compounds of different chemical classes. In a first step, the CSD database was searched for compounds containing OHO hydrogen bonds with known neutron diffraction structure. From these compounds those were selected which fulfill the following criteria:

- Simple structure with easily resolvable hydrogen position inside the hydrogen bond.
- The temperature of the neutron diffraction examination should be as low as possible to prevent the proton from oscillating between the two oxygens and thus have an intermediate position that is not the original position below the thermal activation.
- The substances are allowed to have non-linear hydrogen bonds so that the selection of the substances is more 'real world' like and not restricted to special cases. Although this would enlarge the scatter of the data these substances are included.

According to these considerations the compounds collected in Table 1 were chosen.

Table 1
Hydrogen bonded solids whose low-temperature neutron diffraction data are available in the Cambridge Structural Database (CSD) and which were studied by high-resolution solid state ^{1}H NMR. ^{1} H chemical shifts measured by us.

Substance and CSD code	Structure	Class	q_1	q_2	r_{OO}	^{1}H (ppm)	Values obtained by Harris [28]
3-Deazaauracil CAXKOB11	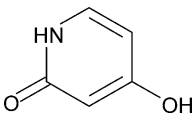	Amides and amino acids	0.2630	2.602	2.599	13.5	
Benzoic acid BENZAC09	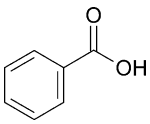	Carboxylic acids (aromatic)	0.3115	2.609	2.606	12.9	12.7
Benzoylacetone BZOYAC04 compound **2** in Figs. 4,5	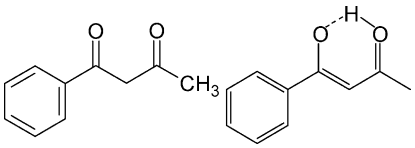	*cis*-Keto–enol-tautomeres	0.0425	2.575	2.502	16.2	
Succinic acid SUCACB03	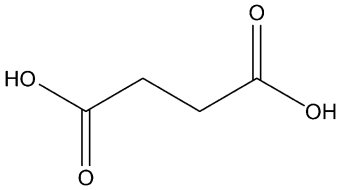	Carboxylic acids and salts	0.3350	2.670	2.673	12.8	
Dibenzoylmethane DBEZLM02 compound **1** in Figs. 4,5	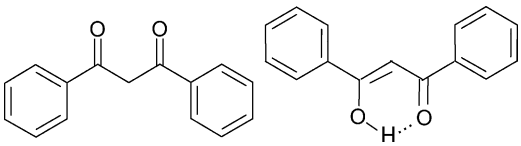	*cis*-Keto–enol tautomeres	0.1005	2.521	2.495	18.1	
DL-Serine DLSERN11	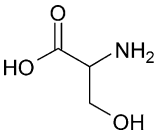	Amides and amino acids	0.3460	2.692	2.679	08.6	
DL-Tartaric acid TARTAC01	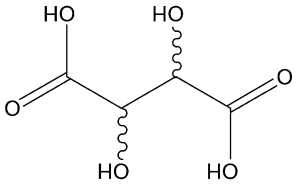	Carboxylic acids and salts	0.3170 0.3515 0.4345 0.4860	2.636 2.719 2.845 2.922	2.630 2.705 2.837 2.901	12.4 10.8 06.7 04.5	12.7 11.7 7.0
Ferrocene 1,1′dicarboxylic acid FEROCA12	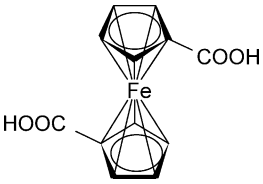	Organometalls	0.2925	2.601	2.600	13.7	
Ibuprofen IBPRAC01	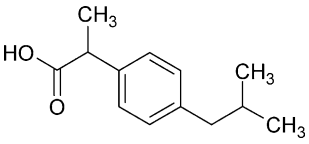	Carboxylic acids (aromatic)	0.3500	2.626	2.626	12.1	

(*continued on next page*)

Table 1 (*continued*)

Substance and CSD code	Structure	Class	q_1	q_2	r_{OO}	^{1}H (ppm)	Values obtained by Harris [28]
Suberic acid SUBRAC03	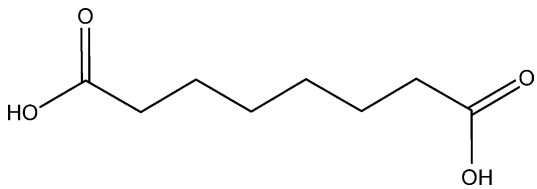	Carboxylic acids and salts	0.3125	2.643	2.642	13.3	
L-Glutamic acid LGLUAC03	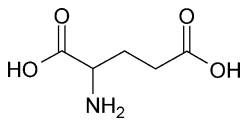	Amides and amino acids	0.2720	2.592	2.581	16.0	16.3
N-Acetylglycine ACYGLY11	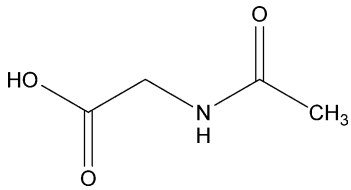	Amides and amino acids	0.2475	2.563	2.562	15.6	
N-Acetyl-L-cysteine NALCYS02	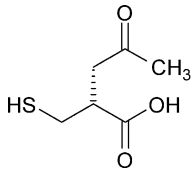	Amides and amino acids	0.2385	2.549	2.549	14.9	
Naphtazarin C (5,8-Dihydroxy-1,4-naphthoquinone) DHNAPH17	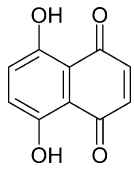	*cis*-Keto–enol tautomeres	0.3305 0.3405	2.681 2.667	2.583 2.570	12.4 12.4	
Sodium hydrogen maleate NAHMAL01 compound **3** in Fig. 4,5	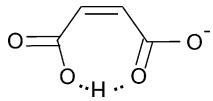	Carboxylic acids and salts	0.1440	2.446	2.445	19.1	
Paracetamol HXCAN19	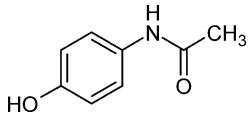	Amides and amino acids	0.3745	2.667	2.660	09.3	
p-Nitrobenzoic acid NBZOAC06	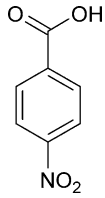	Carboxylic acids (aromatic)	0.3550	2.646	2.626	13.0	
Squaric acid KECYBU13	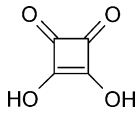	Carboxylic acids and salts	0.2495	2.547	2.547	14.6	
Salicylic acid SALIAC12	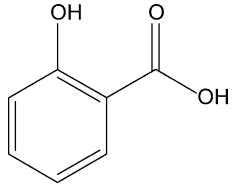	Carboxylic acids (aromatic)	0.3325 0.4060	2.637 2.720	2.637 2.608	12.2 09.6	12.3 9.8

The codes refer to the CSD.

1.2. Experimental section

The data were obtained, using a Varian 600 MHz InfinityPlus NMR spectrometer running the Spinsight software (version 4.3.2), employing 3.2 and 2.5 mm Chemagnetics HX-T3 probes. The MAS speed was set to 24 kHz, if not otherwise noted. (Exceptions: benzolyacetone was measured using only 22 kHz; *N*-acetylglycine was measured on a Varian 300 MHz InfinityPlus NMR spectrometer using a 4 mm Bruker ^{1}H probe and 12 kHz MAS-frequency.) The measurements were made at room temperature without additional cooling. All spectra were referenced against TSP (Tetramethylsilyle propionic acid, Na salt) as an external chemical shift standard. The repetition times of the experiments were chosen in such a way that all spectra were fully relaxed.

To suppress the considerable proton background signal of the probes, all spectra were recorded employing a rotor synchronized Hahn–Echo sequence with delay times between 800 μs and 3 ms. The delay times were chosen as an optimized compromise between the signal decay owing to relaxation and the resolution gain owing to longer delay times.

2. The valence bond order model

To a given hydrogen bond of the type A–H···B one can normally associate distances, r_{AH} and r_{HB} for the diatomic units AH and H···B. According to Pauling [21], these distances correspond to the valence bond orders

$$p_{AH} = \exp\{-(r_{AH} - r^0_{AH})/b_1\},$$
$$p_{HB} = \exp\{-(r_{HB} - r^0_{JB})/b_{HB}\}, \text{ with } p_{AH} + p_{HB} = 1. \quad (1)$$

r^0_{AH} and r^0_{HB} are the equilibrium distances of the fictive diatomic molecules AH and HB, and b_{AH} and b_{HB} are the parameters describing the bond order decrease when the distances d_{AH} and d_{HB} are increased. For hydrogen, the total valence has to be unity [18]. This relation leads to a correlation of r_{AH} and r_{HB} [15,17,18]. For OHO-systems (A, B=O) Steiner has proposed the values [15]

$$r^0_{OH} = r^0_{HO} = 0.942 \text{ Å}, \; b = b_{OH} = b_{HO} = 0.371. \quad (2)$$

The correlation of r_{OH} with r_{HO} also implies a correlation of the quantities.

$$q_1 = 1/2(r_{OH} - r_{HO}) \text{ and } q_2 = r_{OH} + r_{HO} \quad (3)$$

q_2 corresponds in the case of linear hydrogen bonds to the heavy atom distance r_{OO}; q_1 is called the hydrogen bond coordinate as it represents in linear hydrogen bonds the deviation of the proton from the hydrogen bond center. The q_2 vs. q_1 correlation can be written as [4]

$$q_2 = r^0_{HO} + r^0_{OH} - b_{OH} \ln(1 - \exp(-(r_{OH} - r^0_{OH})/b_{OH})). \quad (4)$$

Eqs. (3) and (4) give an implicit correlation between the variables q_1 and q_2 as depicted in the graph of Fig. 2. When

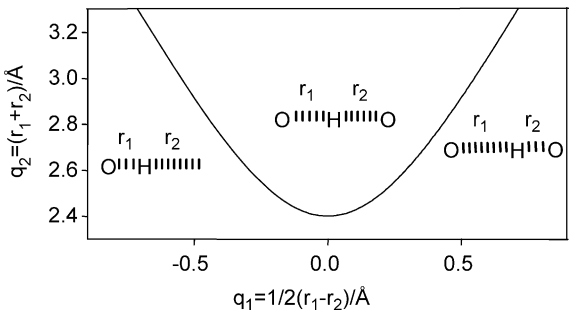

Fig. 2. Hydrogen bond correlation curve for O–H···O hydrogen bonded complexes calculated from Eq. (4). $q_2 = r_1 + r_2$ represents the heavy atom distance in case of a linear hydrogen bridge, $q_1 = 1/2(r_1 - r_2)$ the proton transfer coordinate.

OH and O are far from each other, q_1 exhibits large negative values and the heavy atom separation q_2 large positive values. When the H-bond is formed, the absolute value of q_1 decreases and in the extreme of a symmetric H-bond goes to zero, when it is located in the hydrogen bond center. At the same time, q_2 decreases to a minimum value. Once the proton has crossed the H-bond center, the q_1 values become positive and q_2 increases again, until the hydrogen bond is again broken at large values.

Some of us have found the following correlation between ^{1}H chemical shifts and the bond orders of Eq. (1):

$$\delta(A\underline{H}B) = 4\Delta_{A\underline{H}B} p_{AH} p_{HB} + p_{A\underline{H}}\delta^0_{A\underline{H}} + p_{\underline{H}B}\delta^0_{\underline{H}B} \quad (5)$$

The parameters in this equation have to be established empirically. In principle, they depend on the chemical systems studied. δ^0_{AH} and δ^0_{HB} represent the chemical shifts of the fictive isolated diatomic molecules AH and BH, and Δ_{AHB} the excess term at the configuration with the shortest AHB-hydrogen bond. For the OHO data set of Mc Dermott [8], Schah–Mohammedi [22] found the values of $\Delta_{O\underline{H}O} = 20.5$ and $\delta^0_{OH} = 2$ ppm, whereas for the data set of Sternberg [7], Detering [23] determined a value of $\Delta_{O\underline{H}O} = 22.6$ and $\delta^0_{O\underline{H}} = -1$ ppm. The resulting maximum value of 21.6 ppm corresponds to the value found by Denisov et al. [24] by NMR investigations of stabilized $H_5O_2^+$ in solution at 90 K. Finally, another correlation of liquid NMR measurements done by Tolstoy et al. [36] for carbonic acids leads to comparable results (ΔH determined to 25 ppm and δ^0_{OH} to -4 ppm).

3. Results and discussion

3.1. Experimental results

3.1.1. Resolution enhancement by MAS-echo-spectroscopy

Fig. 3 depicts the typical high-resolution ^{1}H NMR spectra of one of the hydrogen bonded solids studied, i.e. Ferrocene 1,1′-dicarbonic acid. This molecule forms double hydrogen bonded cyclic dimers in the solid state [25]. Fig. 3a shows the normal ^{1}H NMR spectrum obtained under high

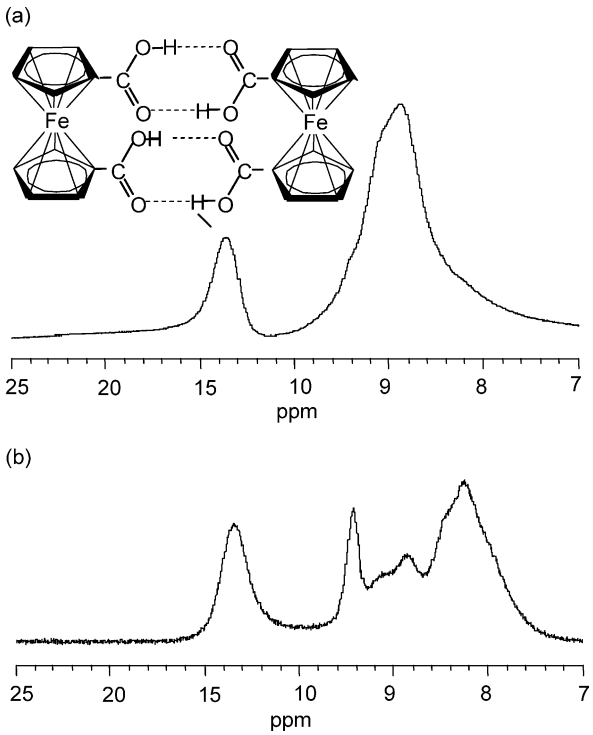

Fig. 3. (a) Normal 600 MHz ^{1}H MAS–NMR spectrum (24 kHz.) of Ferrocene 1,1′-dicarboxylic acid. (b) Rotor synchronized echo MAS spectrum (24 kHz, 832 μs echo delay). Note the vast improvement of resolution.

MAS and 90° irradiation, and Fig. 3b the rotor synchronized echo spectrum obtained under the same conditions. The large background signal and the base line distortions in the center of the lines of Fig. 3a are partially due to proton background signal of the probe and partially due to strongly dipolar coupled proton spins. In comparison, the echo spectra of Fig. 3b exhibits a far superior baseline, where the lines of the relevant protons inside the molecule are nicely resolved. Thus, by simple inspection of the spectra it is evident that the resolution of the echo MAS spectra is strongly improved as compared to the normal MAS–FID spectrum.

3.1.2. Proton chemical shifts extracted from the echo spectra

In the next step the ^{1}H chemical shifts of the protons inside the hydrogen bonds were extracted from the echo spectra. For this purpose the resonance of the hydrogen-bonded proton had to be identified and assigned. As the hydrogen bonded protons are expected to exhibit the largest chemical shift of all lines in each of the spectra, this assignment is rather simple. The analysis of the experimental results was done in two steps. In the first step, the chemical shift values of the individual hydrogen bonded proton were determined and these values then plotted in the second step as a function of the distance q_1 obtained from the low-temperature neutron diffraction data in the CSD. In the following, we discuss certain systems in more detail, characterized by an increasing complexity of their ^{1}H NMR spectra. All data obtained are assembled in Table 1.

Benzoylacetone and *dibenzoylmethane* are keto–enol tautomers exhibiting a strong intramolecular hydrogen bond. The q_1 values are smaller than those of the other compounds. The hydrogen bonded protons exhibit chemical shifts of 16.2 ppm in the case of benzoylacetone and 18.1 ppm in the case of dibenzoylmethane. The ^{1}H signals are well separated from the aliphatic and aromatic signals of the remaining protons (spectra not shown). We will discuss the unusual properties of these two systems later.

Naphtazarin C exhibits two short intramolecular hydrogen bonds with a geometry similar to the keto–enol tautomers, benzoylacetone and dibenzoylmethane. Owing to the high symmetry of the molecule, reflected in the very similar hydrogen bond positions, which differ only by 2/100th of an Angstrom, both hydrogen atoms are indistinguishable in the ^{1}H NMR spectrum and contribute to a single line at 12.4 ppm. This line is well separated from the aromatic protons visible as a signal around 7 ppm (spectra not shown). This compound has been studied previously by Fyfe et al. using ^{13}C CPMAS NMR, where an asymmetric structure was observed in a low-temperature phase, but a symmetric structure in the room temperature phase [26]. ^{1}H solid state relaxation measurements on static powders were performed by Medycki et al. from which information about the dynamics of the proton transfers were obtained [27].

The carboxylic acids benzoic acid, succinic acid, ibuprofen, suberic acid and *para*-nitro benzoic acid all exhibit only a single type of hydrogen bond with intermediate strength and thus hydrogen bond length in their crystal structure. These compounds form hydrogen-bonded dimers with two identical hydrogen bonds, where the dicarboxylic acids form band like structures. Their dispersion of the overall length is very small and nearly all of the selected substances are found in the region of 2.6 Å (q_2). All protons inside the hydrogen bonds have similar chemical shifts between 12 and 13 ppm (Table 1) and relative sharp signals that are well separated from the aliphatic or aromatic signals (spectra not shown). These values compare well with the value of 12.7 ppm, which was identified by Harris [28] as the peak for the hydrogen bonded proton in benzoic acid dimer.

Squaric acid contains only two equivalent protons, which are both part of strong hydrogen bonds with an overall O···O distance (q_2) of 2.55 Å and a proton deviation from the hydrogen bond's center (q_1) of 0.250 Å. The resulting spectrum is very simple and consists of a single peak at 14.6 ppm (spectra not shown). This value is slightly higher than the signals of the carbonic acids and can be explained by the shorter hydrogen bonds compared to the other carbonic acids. The crystal structure of this molecule was studied recently as a function of pressure by Katrusiak [29].

Ferrocene 1,1′ dicarboxylic acid forms—in contrast to the 'normal' dicarboxylic acids—cyclic hydrogen bonded

dimers with two different O···O distances of 2.600 Å (q_2 = 2.601) and 2.626 Å (q_2 = 2.632) and bond angles of 176.1° and 178.4°. The nearly ecliptic pentadiene rings are coordinated to an iron atom and two molecules of ferrocene dicarboxylic acid are connected via four hydrogen bonds, which are pair wise identical. The strength of the hydrogen bonds is higher than in normal carbonic acids. They both resonate in a single line at 13.4 ppm, which cannot be further resolved in the ^{1}H MAS–NMR spectrum (Fig. 3).

Salicylic acid forms dimers similar to those found for the carboxylic acids and additionally another hydrogen bond to the protons of the (*ortho*-) hydroxyl group. In this way, a longer (linear, q_2 = 2.72 Å) and a shorter (non-linear, q_2 = 2.64 Å) hydrogen bond are formed and can be separated in the solid state ^{1}H MAS–NMR spectrum. The stronger hydrogen bond is found for the protons of the carboxy groups, which connect the molecules to dimers. They resonate at 12.2 ppm (spectra not shown). The signal of the proton in the hydroxy group, which forms the weaker hydrogen bond, is found at 9.6 ppm. This is close to the aromatic protons and causes a partial overlap with their lines.

DL-Tartaric acid in the crystal has four intermolecular hydrogen bonds of different strength. Their q_1 values range from 0.317 to 0.486 Å and their q_2 values from 2.6 to 2.9 Å. In contrast to the normal dicarboxylic acids, the two hydrogen bonds from the carboxyl group are of different lengths. The four hydrogen bonds are clearly distinguishable in the ^{1}H MAS–NMR spectrum, since the strength of the bonds is different and so the protons of the hydrogen bonds can be attributed to the lines according to their q_1 values (for clarity the atom numbers are given here since the explanation would be otherwise too complicated). The shortest hydrogen bond has a chemical shift of 12.4 ppm (spectra not shown). This hydrogen bond from a carboxy group to one of the hydroxyl groups has an overall bond length of 2.636 Å (O2–H4–O4). The second intermolecular hydrogen bond at 10.8 ppm with a q_2 distance of 2.719 Å (O5–H6–O3) is between the carboxylic oxygen to the proton of the second molecule's carboxy group. The third intermolecular hydrogen bond can be found at 6.7 ppm (O1–H3–O6) and connects a hydroxyl group to another molecules carboxylic oxygen. The smallest chemical shift is found for the longest hydrogen bond with a (q_2) distance of 2.922 Å, connecting a hydroxyl group to the other carboxylic oxygen (O4–H5–O3).

Sodium-hydrogen-maleate forms a very complex hydrogen bond pattern, which to a large extend is influenced by crystal water. Three of the hydrogen bonds are between the carboxylate anion and one single water molecule; the fourth is connected to a different water molecule. The intramolecular hydrogen bond between the protonated acid function and a carboxylic oxygen is very short (q_2 = 2.446 Å) and the proton is located close to the center of the hydrogen bond. For maleic acid, mono-Na salt, only one of the obtained values was used for the correlation of the chemical shift vs. q_1. The reason is, that we don't have the possibility to control the water content of the sample and since the hydrogen bonds are mainly between the water molecules in the crystal (the bonds' distances will be changed by a different water content and so the high quality neutron crystal structure is useless), only the hydrogen bond with the lowest influence of crystal water (this is the shortest hydrogen bond) was selected. The ^{1}H MAS–NMR spectrum shows six resolved signals and the shortest hydrogen bond shows a signal at 19.1 ppm (spectra not shown).

Paracetamol (p-hydroxyphenylacetamid) forms crystals with a medium OHO hydrogen bond (2.677 Å) and a longer NHO bond of nearly 3 Å. Both, the phenolic OH group and the NH group form hydrogen bonds to the carbonyl oxygen. The proton of the OHO bond is shifted slightly more from the center of the hydrogen bond (q_2 = 2.677 Å O1–H5–O2, q_1 = 0.3765 Å) than in plain carboxylic acid dimers with a chemical shift of 9.3 ppm (spectra not shown). The NHO hydrogen bond was not further considered. The crystal structure of this molecule was studied recently as a function of pressure by Boldyreva et al. [30].

The situation for *N-acetylglycin* is similar to the situation in paracetamol. Here, too, a shorter OHO bond and a longer NHO hydrogen bond are visible in the crystal structure. The OHO hydrogen bond is shorter than the one in paracetamol (q_2 = 2.563 Å, q_1 = 0.2475, O1–H4–O3) and has a chemical shift of 15.6 ppm (spectra not shown). The spectrum was recorded using the 300 MHz InfinityPlus spectrometer at 12 kHz MAS speed, which results in the relatively low resolution.

N-Acetyl-L-cystein contains only one OHO-hydrogen bond from the hydroxyl group to the carboxylic acid's oxygen in the crystal structure. The overall length of this hydrogen bond is shorter than the analogue hydrogen bond in *N*-acetylglycine and the proton has a chemical shift of 14.9 ppm (q_2 = 2.549).

The crystal structure of *3-deazauracile* exhibits two intermolecular hydrogen bonds. The OHO hydrogen bond (q_2 = 2.602 Å, q_1 = 0.2630 Å) is slightly shorter than the OHO hydrogen bond of paracetamol and has a chemical shift of 13.5 ppm (spectra not shown).

Next, the examined amino acids are discussed. Since, these amino acids are in a zwitterionic state, there are more NHO hydrogen bonds, due to the protonation of the $-NH_2$ group. Compared to the substances mentioned above, all intermolecular hydrogen bonds occur between the $-NH_3^+$ group and the carboxylate ion.

DL-Serine exhibits four different hydrogen bonds in its crystal structure. Three of the hydrogen bonds have their origin in the protonated amino group and end in the carboxylate rest. The OHO hydrogen bond has an overall length of 2.692 Å (q_1 = 0.3460 Å) and is shorter than the NHO hydrogen bonds with lengths between 2.8 and 2.9 Å. The highest chemical shift with 8.6 ppm is connected to the OHO hydrogen bond (spectra not shown).

L-Glutamic acid contains only one OHO hydrogen bond. With 2.592 Å ($q_1 = 0.2720$ Å) it is shorter than the three NHO hydrogen bonds, which range between 2.8 and 2.9 Å in length and are thus of the same length as those observed in DL-Serine. The chemical shift of the OHO hydrogen bond of glutamic acid is determined as 16.0 ppm (spectra not shown).

4. Discussion

The analysis of the geometrical information obtained from the neutron scattering data has shown, that there are two possibilities to correlate the geometric parameters of hydrogen bonds. Previously, r_{AH} was correlated with r_{AB} [14], but Steiner et al. [15–17] showed that the correlation of r_{AH} with r_{HB} is more exact. Furthermore, this correlation is supported theoretically by the empirical valence bond order concept. Equivalent is the correlation of q_2 vs. q_1. We have plotted in Fig. 4 this correlation obtained for the OHO-hydrogen bonds of the compounds studied here by high-resolution NMR, for which neutron diffraction data were available in the CSD. We confirm that the scattering of the data of the q_2 vs. q_1 correlation is much smaller as compared to the corresponding r_{OH} vs. r_{OO}.

As explained above, the resulting curve resembles the pathway of the protons moving to the center of a hydrogen bond. In order to visualize this pathway we have plotted the data points in Fig. 4 twice, centro symmetric about the origin at $q_1 = 0$, because in hydrogen bonds of the type AHA the choice of the distance r_{AH} and r_{HA} is arbitrary, as it was done previously in the case of the NHN-systems [4]. We note deviations of compounds **1** and **2** from the correlation line, whereas **3** is well located on the curve. We will discuss this interesting behavior below in more detail. (Fig. 5)

In Fig. 6, we have plotted the experimentally determined chemical shift of the hydrogen bonded protons as a function of q_1. The solid line was calculated using Eq. (5). The following parameters were obtained by eye fitting:

$$\Delta(O\underline{H}O) = 22.6 \text{ ppm and } \delta^0_{O\underline{H}} = -1 \text{ ppm}.$$

The values for weak and intermediate hydrogen bonds are in excellent agreement with the correlation line, and deviations will reflect chemical influences on the chemical shifts. The parameters obtained are identical to those obtained by Detering [23] for the data set of Brunner et al. [11] and very close to the parameters obtained by Schah–Mohammedi [22] for the data set of McDermott [8]. Since the range of compounds in the present study covers a much larger number of different classes of compounds, it is evident that these parameters seem to exhibit a universal character, where the scattering of the data arises mainly from secondary structural effects.

Again, similar to Fig. 4, we observe strong deviations for **1** and **2**, whereas **3** is again well located on the correlation line. These deviations are not caused by the different temperatures where neutron diffraction data and ^{1}H NMR data were obtained, as they are present in Fig. 4 as well as in Fig. 5. These deviations can be explained as follows. The q_2 values of both compounds are too large for the value of q_1 observed in the neutron diffraction data, if we assume the validity of the hydrogen bond correlation. In addition, the ^{1}H chemical shifts of the hydrogen bonded protons are not as large as expected for such small values of q_1. It is well known that six-membered H-chelate rings of the malonaldehyde type as present in the enol forms of **1** and **2** exhibit a double well potential for the proton motion, where the proton is either delocalized or moves rapidly [31,32] between two tautomeric states, as it is indicated in Scheme 1 and Scheme 2 of Fig. 5. Solid state interactions lift the symmetry between the two tautomers, and one of them is normally favored. If the proton wave function is broad, neutron diffraction will not recognize

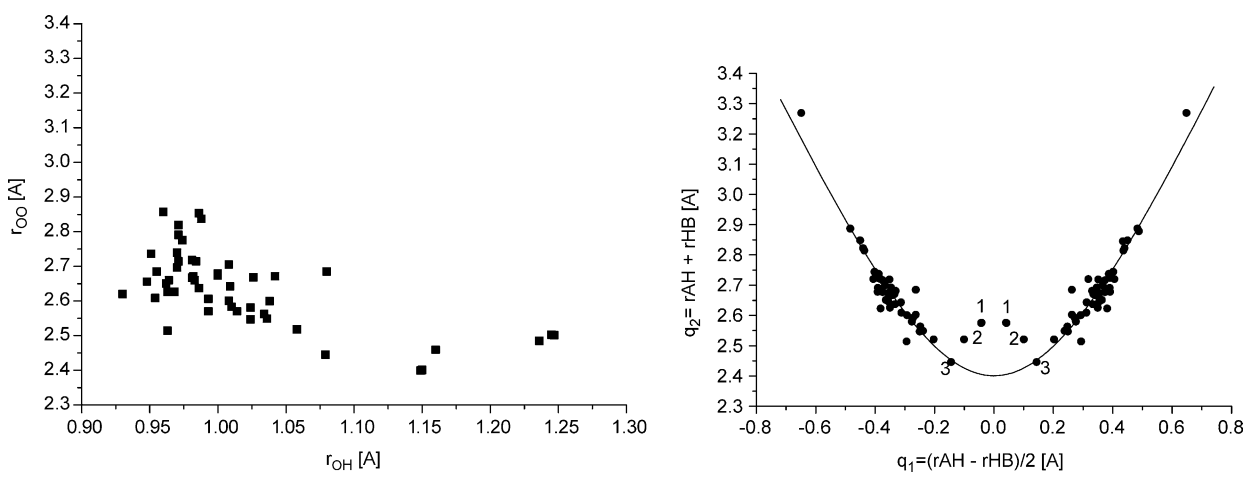

Fig. 4. Comparison between two correlations using the 'through space' (left) and the 'through bond' (right) distance as heavy atom distances. The right graph shows much less scattering of the data in particular for the weak hydrogen bonds.

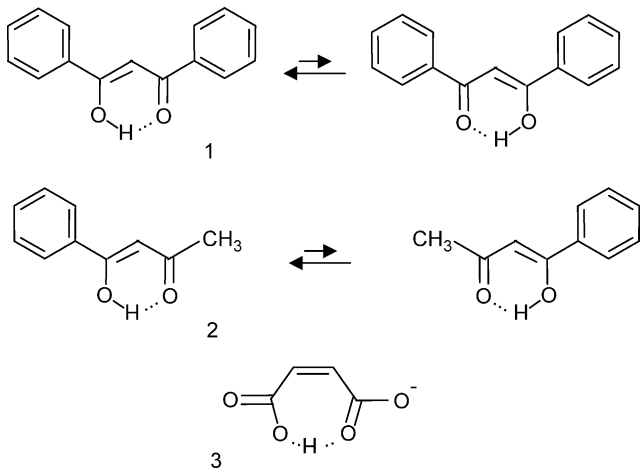

Fig. 5. The keto–enol tautomers **1** (Dibenzoylmethane) and **2** (Benzoylacetone) do not fit into the theoretical curve in Fig. 4, whereas **3** (maleic acid, mono Na salt) fits perfectly.

the tautomerism. Because of the small asymmetry of the proton potential, q_1 is not found to be zero. An asymmetry caused by solid state interactions is smaller than those caused by a chemical asymmetry. Hence, the absolute q_1 values of **2** are larger than those of **1**.

On the other hand, the maleate anion **3** which is located on both correlation curves of Figs. 4 and 5, is known to exhibit a single well potential for the proton motion [33,34]. Also, the solid state will lift the symmetry of the anion and hence, values of q_1 which are non-zero will arise.

Finally, we wish to note that the combination of fast ^{1}H MAS–NMR spectroscopy with echo detection allows a much easier faithful detection of the ^{1}H chemical shifts of the proton in the OHO hydrogen bond than the previous ^{1}H-CRAMPS NMR studies. Thus, this technique allows fast and simple characterization of OHO-hydrogen bonds, which in the future can be applied to systems where no neutron crystal structure is available.

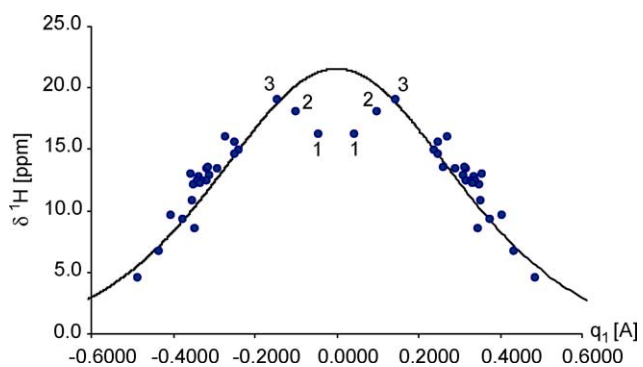

Fig. 6. Correlation of the experimentally obtained chemical shift with the deviation of the proton from the center of the hydrogen bond (q_1). The experimental data are plotted as dots, the solid line is a fit of the experimental points employing the valence bond model. The uncertainty of the measured chemical shift is around 0.1 ppm and is resembled by the point size in the correlation. To separate different q_1 values their difference must be larger than 2/100th of an Angstrom.

5. Summary and conclusion

Based on neutron diffraction data of crystal structures, a selection of several substances of different chemical classes with OHO hydrogen bonds and known neutron diffraction structure was studied employing fast ^{1}H MAS–NMR methods. It is shown that by the application of a simple rotor synchronized echo sequence in combination with fast MAS, it is possible to faithfully determine the chemical shift of the proton. This chemical shift is correlated to the deviation of the proton from the center of the hydrogen bond. Deviations from the correlation curves arise in cases of non-recognized proton delocalization in hydrogen bonds exhibiting a small barrier for the proton motion. Thus, it is now possible to routinely determine the position of the proton in a hydrogen bond, independently of the solubility or crystallizability of a compound, employing a simple ^{1}H-fast MAS–NMR experiment and the correlation curve obtained, respectively, extended in this work.

In the future, a task will be to improve the theoretical basis for the so far empirical valence bond order model and to take hydrogen bond proton delocalization into account. In the meantime, the deviations are of highly diagnostic value, as they identify compounds worth to study in more detail using other techniques. Such a technique, which has not yet been mentioned, is the correlation of NMR chemical shift data and quadrupolar couplings for deuterium. Here, the database can be even further extended employing many available X-ray diffraction data, which faithfully localize the deuterium position in the hydrogen bond. This technique allows one to do low-temperature measurements down to 10 K, which will strongly improve the overlap between neutron diffraction and NMR in the future. Such experiments are currently in progress in our lab.

Acknowledgements

We acknowledge the financial support of the Deutsche Forschungsgemeinschaft (DFG) via the Collaborative Research Center 498, DFG Research Training Center 788 and the Fonds der Chemischen Industrie, Frankfurt.

References

[1] G.A. Jeffrey, W. Saenger, Hydrogen Bonding in Biological Structures, Springer, Berlin, 1991.
[2] (a) J.E. Roberts, G.S. Harbison, M.G. Munowitz, J. Herzfeld, R.G. Griffin, J. Am. Chem. Soc. 109 (1987) 4163.
(b) P. Tekely, F. Montigny, F. Canet, J. Delpuech, J. Chem. Phys. Lett. 175 (1990) 401.
(c) M.G. Munowitz, R.G. Griffin, J. Chem. Phys. 76 (1982) 2848.
(d) M.G. Munowitz, W.P. Aue, R.G. Griffin, J. Chem. Phys. 77 (1982) 1686.
[3] C.G. Hoelger, H.-H. Limbach, J. Phys. Chem. 98 (1994) 11803.

[4] (a) H. Benedict, H.-H. Limbach, M. Wehlan, W.-P. Fehlhammer, N.S. Golubev, R. Janoschek, J. Am. Chem. Soc. 120 (1998) 2939.
(b) G. Buntkowsky, I. Sack, H.-H. Limbach, B. Kling, J. Fuhrhop, J. Phys. Chem. B 101 (1997) 11265.
(c) I. Sack, S. Macholl, F. Wehrmann, J. Albrecht, H.H. Limbach, F. Fillaux, M.H. Baron, G. Buntkowsky, Appl. Magn. Reson. 17 (1999) 413.
[5] P. Lorente, I.G. Shenderovich, G. Buntkowsky, N.S. Golubev, G.S. Denisov, H.-H. Limbach, Magn. Reson. Chem. 39 (2001) 18.
[6] I. Sack, A. Goldbourt, S. Vega, G. Buntkowsky, J. Magn. Reson. 138 (1999) 54.
[7] U. Sternberg, E.L. Brunner, Magn. Reson. A 108 (1994) 142.
[8] A. McDermott, C.F. Ridenour, Encyclopedia of NMR, Wiley, Sussex, UK, 1996.
[9] A.S. Mildvan, T.K. Harris, C. Abeygunawardana, Meth. Enzymol. 308 (1999) 219.
[10] T.K. Harris, A.S. Mildvan, Proteins 35 (1999) 275.
[11] E. Brunner, U. Sternberg, J. Prog. NMR Spectrosc. 32 (1998) 21.
[12] S.N. Smirnov, H. Benedict, N.S. Golubev, G.S. Denisov, M.M. Kreevoy, R.L. Schowen, H.H. Limbach, Can. J. Chem. 77 (1999) 943.
[13] I.G. Shenderovich, P.M. Tolstoy, N.S. Golubev, S.N. Smirnov, G.S. Denisov, H.H. Limbach, J. Am. Chem. Soc. 125 (2003) 11710.
[14] (a) S.W. Peterson, H.A. Levy, S.H. Simonsen, J. Chem. Phys. 21 (1953) 2084.
(b) I. Olovsson, P.G. Jonsson, P. Schuster, G. Zundel, C. Sandorfy,The Hydrogen Bond, Recent Developments in Theory and Experiments-North-HollandAmsterdam (1976) 394–455.
[15] T. Steiner, W. Saenger, Acta Crystallogr. Sect. B 50 (1994) 348.
[16] T. Steiner, J. Chem. Soc. Chem. Commun. (1995) 1331.
[17] T. Steiner, J. Phys. Chem. A 102 (1998) 7041.
[18] I.D. Brown, Acta Crystallogr. Sect. B 48 (1992) 553.
[19] M. Ramos, I. Alkorta, J. Elguero, N.S. Golubev, G.S. Denisov, H. Benedict, H.H. Limbach, J. Phys. Chem. A 101 (1997) 9791.
[20] O. Picazo, I. Alkorta, J. Elguero, J. Org. Chem. 68 (2003) 7485.
[21] (a) L. Pauling, J. Am. Chem. Soc. 69 (1947) 542.
(b) I.D. Brown, Acta Crystallogr. B 48 (1992) 553.
[22] P. Schah-Mohammedi, NMR Studies on the Geometry of Low Barrier Hydrogen Bonds in Acid Base Complexes, PhD Thesis, FU Berlin, Department of Chemistry, 2001.
[23] C. Detering, NMR Studies of Strong H-Bonds in Complexes involving Phosphoric Acids in Solution, PhD Thesis, FU Berlin, Department of Chemistry, 2001.
[24] N.S. Golubev, Khim. Fiz. 3 (1984) 772.
[25] CSD Code FEROCA12.
[26] W.I. Shiau, E.N. Duesler, I.C. Paul, D.Y. Curtin, W.G. Blann, C.A. Fyfe, J. Am. Chem. Soc. 102 (1980) 4546.
[27] W. Medycki, E.C. Reynhardt, L. Latanowicz, Mol. Phys. 93 (1998) 323.
[28] R.K. Harris, P. Jackson, L.H. Merwin, Chem. Soc. Faraday Trans. 1 84 (1988) 3649.
[29] A. Katrusiak, Phys. Rev. B 48 (1993) 2992.
[30] E.V. Boldyreva, T.P. Shakhtshneider, M.A. Vasilchenko, H. Ahsbahs, H. Uchtmann, Acta Crystallogr. B 56 (2000) 299.
[31] M.R. Johnson, N.H. Jones, A. Geis, A.J. Horsewill, H.P. Trommsdorff, J. Chem. Phys. 116 (2002) 5694.
[32] U. Langer, L. Latanowicz, C. Hoelger, G. Buntkowsky, H.M. Vieth, H.H. Limbach, Phys. Chem. Chem. Phys. 3 (2001) 1446.
[33] (a) C.L. Perrin, J.B. Nielson, J. Am. Chem. Soc. 119 (1997) 12734.
(b) C.L. Perrin, Science 266 (1994) 1665.
(c) D. Madsen, C. Flensburg, S. Larsen, J. Phys. Chem. A 102 (1998) 2177.
(d) M. Garcia-Viloca, A. Gonzalez-Lafont, J.M. Lluch, J. Am. Chem. Soc. 121 (1999) 9198.
[34] P. Schah-Mohammedi, I.G. Shenderovich, C. Detering, H.H. Limbach, P.M. Tolstoy, S.N. Smirnov, G.S. Denisov, N.S. Golubev, J. Am. Chem. Soc. 122 (2000) 12878.
[35] (a) B.C. Gerstein, R.G. Pembleton, R.C. Wilson, L.M. Ryan, J. Chem. Phys. 66 (1977) 361.
(b) B.C. Gerstein, Advances in colloid and interface, Science 23 (1985) 45.
(c) C.E. Bronnimann, B.L. Hawkins, M. Zhang, G.E. Maciel, Anal. Chem. 60 (1988) 1743.
[36] H.H. Limbach, M. Pietrzak, H. Benedict, P.M. Tolstoy, N.S. Goluber, G.S. Denisov, J. Mol. Struct. this issue.